Terahertz-Field-Induced Large Macroscopic Polarization and Domain-Wall Dynamics in an Organic Molecular Dielectric

T. Morimoto, T. Miyamoto, H. Yamakawa, T. Terashige, T. Ono, N. Kida, and H. Okamoto
Department of Advanced Materials Science, University of Tokyo, Kashiwa 5-1-5, Chiba 277-8561, Japan
(Received 23 May 2016; published 10 March 2017)

A rapid polarization control in paraelectric materials is important for an ultrafast optical switching useful in the future optical communication. In this study, we applied terahertz-pump second-harmonic-generation-probe and optical-reflectivity-probe spectroscopies to the paraelectric neutral phase of an organic molecular dielectric, tetrathiafulvalene-*p*-chloranil and revealed that a terahertz pulse with the electric-field amplitude of ∼400 kV/cm produces in the subpicosecond time scale a large macroscopic polarization whose magnitude reaches ∼20% of that in the ferroelectric ionic phase. Such a large polarization generation is attributed to the intermolecular charge transfers and breathing motions of domain walls between microscopic neutral and ionic domains induced by the terahertz electric field.

DOI: 10.1103/PhysRevLett.118.107602

Recent developments of femtosecond laser technology enable us to generate an intense terahertz electric-field pulse, the amplitude of which is far beyond 100 kV/cm. Such a strong electric field can be used for the control of electronic properties in solids [1–13]. Typical examples are the insulator-metal transition in a correlated-electron oxide, VO_2 [6] and the modifications of the spin structures in a multiferroic, $TbMnO_3$ [10]. In the viewpoint of optical-property controls, a modulation of polarization amplitudes in dielectrics is another important subject. It is because a rapid polarization modulation can be used for putting a high-density signal on light transmitted in the dielectric in the optical communication. Very recently a subpicosecond modulation of ferroelectric polarization by a terahertz electric-field pulse was demonstrated in ferroelectric phases of organic molecular compounds, tetrathiafulvalene-*p*-chloranil (TTF-CA) and $\alpha-(ET)_2I_3$ [ET: bis(ethylenedithio)tetrathiafulvalene] [8,13] and a transition metal oxide, $BiFeO_3$ [12]. In contrast to those successes of ferroelectric-polarization controls, a generation of macroscopic polarization in a paraelectric material by a terahertz electric field has not been achieved yet; it is nevertheless important since a field-induced polarization generation associated with an instability to the ferroelectric phase would cause a large third-order optical nonlinearity, which can realize an ultrafast optical switching useful also for the optical communication. As a stage to achieve such a new type of the polarization control, in our study, we select the paraelectric neutral phase of TTF-CA and aim to generate large macroscopic polarization by a terahertz pulse.

In TTF-CA, the sequential arrangement of donor (D) TTF molecules and acceptor (A) CA molecules leads to the formation of quasi-one-dimensional (1D) electronic states along the a axis [Figs. 1(a)–1(c)] [14]. The electronic state of this compound is characterized by the degree of charge transfer (CT) ρ from A to D molecules [15]. At room temperature, TTF-CA is a neutral van der Waals crystal; because of the overlap of molecular orbitals between D and A molecules, ρ is not zero but ~ 0.3 (ρ_N). Upon lowering the temperature to $T_c = 81$ K, a phase transition occurs to an ionic phase with $\rho \sim 0.6$ (ρ_I) [16–18]. This ionic phase is stabilized by the energy gain resulting from the long-range Coulomb attractions overcoming the ionization

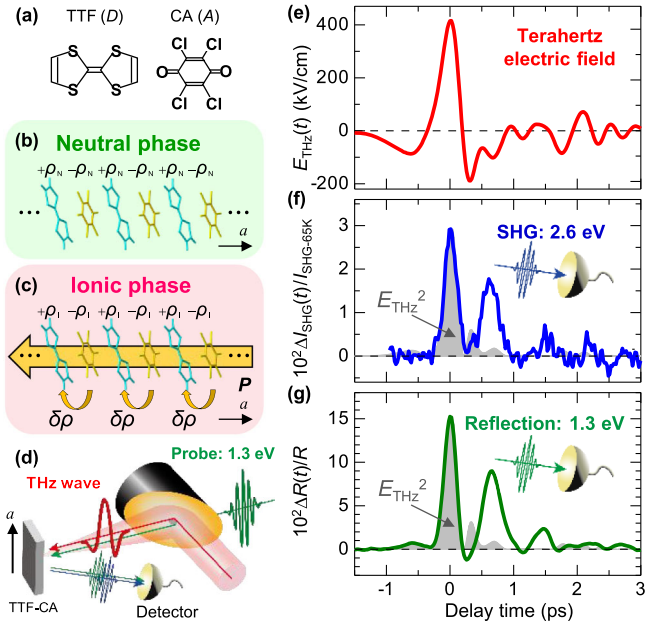

FIG. 1. (a) Molecular structures of TTF and CA. (b),(c) 1D molecular stacks in the neutral phase (b) and the ionic phase (c). P is the spontaneous polarization. (d) Schematic setups of terahertz-pump SHG probe and optical-reflectivity-probe measurements. (e) A waveform of the terahertz electric field $E_{THz}(t)$. (f) A time evolution of the SH intensity at 90 K normalized by the SH intensity at 65 K ($\Delta I_{SHG}(t)/I_{SHG-65\ K}$). (g) A time evolution of $\Delta R(t)/R$ at 90 K. Shaded areas in (f) and (g) show $[E_{THz}(t)]^2$.

energy of the *DA* pairs. In the ionic phase, an unpaired electron exists in each molecule and then the *DA* molecules are dimerized because of the spin-Peierls mechanism. In addition, the dimeric molecular displacements are three-dimensionally ordered and the inversion symmetry is lost [17]. Recent x-ray and theoretical studies revealed that spontaneous polarization with $P_I \sim 6\ \mu\mathrm{C/cm^2}$ along the a axis is produced by fractional charge transfers (CTs) of magnitude $\delta\rho \sim 0.2$ from the A to the D molecules at T_c [19–21]. Thus, the ferroelectric polarization originates not from the displacements of ionic molecules but from the electron-distribution changes. This ferroelectricity is categorized into "electronic ferroelectricity," which is different from conventional displacive and order-disorder types [22]. Therefore, in the paraelectric neutral phase, we can expect that a terahertz electric-field pulse would generate a macroscopic polarization via collective intermolecular CTs.

Single crystals of TTF-CA were grown from the purified TTF and CA microcrystals using the co-sublimation method [23]. In the pump-probe measurements, a Ti:sapphire regenerative amplifier (the central wavelength of 800 nm, the pulse width of 70 fs, the repetition rate of 1 kHz, and the pulse energy of 4 mJ) was used as the light source. The output from the regenerative amplifier was divided into two beams. One was used for the generation of terahertz pulses by the optical rectification process in a $LiNbO_3$ crystal with a tilted-pump-pulse-front method [24]. The electric-field waveform $[E_{\mathrm{THz}}(t)]$ of the generated terahertz pulse was measured by an electro-optical sampling technique. The other beam was used as the excitation source of an optical parametric amplifier, from which probe pulses ranging from 1.1 to 1.5 eV were obtained. The delay time t of the probe pulse relative to the pump pulse was controlled by changing the path length of the probe pulse. The time origin ($t = 0$) is set to be the time of the maximum terahertz electric field. All the measurements were performed on the ab plane of the single crystals.

We begin by detailing the experimental procedure of the terahertz-pump second-harmonic-generation (SHG) probe measurements to detect the macroscopic-polarization generation. First, the sample was cooled down to 65 K and changed to the ferroelectric ionic phase. At that temperature, the probe pulse (1.3 eV) with the electric fields of lights E polarized parallel to the a axis ($E//a$) was incident to the crystal and the intensity of the SH light (2.6 eV), $I_{\mathrm{SHG-65\ K}}$, was measured in the reflection configuration. The SH light was also polarized parallel to a. It was ascertained that $I_{\mathrm{SHG-65\ K}}$ is proportional to the square of the intensity of the incident probe pulse. Next, the temperature was increased up to 90 K and the sample was returned to the neutral phase. At 90 K, the terahertz-pump SHG-probe measurements were performed with the same intensity of the incident probe pulse as that used at 65 K [Fig. 1(d)]. In this procedure, we can compare quantitatively the terahertz-field-induced SH intensity $\Delta I_{\mathrm{SHG-90\ K}}(t)$ in the neutral phase with $I_{\mathrm{SHG-65\ K}}$ in the ionic phase.

By using the terahertz pulse with the electric-field waveform, $E_{\mathrm{THz}}(t)$, which has a maximum value of 415 kV/cm [Fig. 1(e)], we successfully detected the SHG signal $\Delta I_{\mathrm{SHG}}(t)$ at 90 K [Fig. 1(f)]. Near time $t = 0$, $\Delta I_{\mathrm{SHG}}(t)$ exhibits a pulsed response, in good agreement with the square of the terahertz field $[E_{\mathrm{THz}}(t)]^2$ (shaded area). In the ionic phase, the ferroelectric polarization produced by the intermolecular CTs ($\delta\rho \sim 0.2$) activates SHG [8,25]. It is therefore natural to consider that the observed SHG originates from the macroscopic polarization, $\Delta P(t)$, generated also via field-induced CTs, $\Delta\rho(t)$. The initial SH intensity, $\Delta I_{\mathrm{SHG-90\ K}}(0)$, is about 2.9% of the SH intensity at 65 K, $I_{\mathrm{SHG-65\ K}}$. This indicates that the field-induced polarization $\Delta P(0)$ reaches 17% of the polarization $P_I = 6.3\ \mu\mathrm{C/cm^2}$ at 65 K in the ionic phase. After $t = 0.3$ ps, the time evolution of ΔI_{SHG} deviates from the waveform of $[E_{\mathrm{THz}}(t)]^2$ and oscillatory structures appear, which will be discussed later.

To demonstrate a change in ρ by the field-induced CTs, we next focus on the optical reflectivity (R) of the CT band in the near-infrared region, the spectral shape of which is sensitive to ρ [26]. The terahertz-field-induced change in reflectivity $\Delta R(t)/R$ at 1.3 eV (90 K) is shown in Fig. 1(g). In this measurement, both the terahertz pump pulse and the probe pulse are polarized // a. $\Delta R(t)/R$ exhibits a pulsed response at around $t = 0$, which also accords with $[E_{\mathrm{THz}}(t)]^2$ (shaded area). In fact, $\Delta R(0)/R$ is proportional to $[E_{\mathrm{THz}}(0)]^2$ (Supplemental Material S1 [27]). The measurements of the probe-energy dependence of $\Delta R(t)/R$ reveal that the spectral shape of $\Delta R(0)/R$ is in good agreement with the differential reflectivity spectrum between 77 K (the ionic phase) and 90 K (the neutral phase) (Supplemental Material S2 [27]). This demonstrates that ρ is increased by the terahertz electric field and that $\Delta R(t)/R$ at 1.3 eV is a good probe of $\Delta\rho(t)$. This pulsed response is followed by the oscillations and the overall time progression of $\Delta R(t)/R$ is similar to that of $\Delta I_{\mathrm{SHG}}(t)$ [Fig. 1(f)]. This indicates that the fractional CTs [$\Delta\rho(t)$] between D and A molecules are responsible for the polarization $\Delta P(t)$ generated by the terahertz electric field, which is similar to the generation mechanism of the spontaneous polarization in the ionic phase.

To clarify the mechanism of the observed responses in more detail, we measured the temperature dependence of $\Delta R(t)/R$, which is shown in Fig. 2(a). $\Delta R(0)/R$ is enhanced with decreasing temperature [Fig. 2(b)]. Simultaneously, the second peak in $\Delta R(t)/R$ (colored regions) characterizing the oscillation not only increases but also shifts to longer times. This suggests a decrease in the oscillation frequency. Such features cannot be explained by a simple critical behavior associated with the dimerization transition, since the oscillation frequency is much smaller than the dimerization-mode frequency ($\sim 50\ \mathrm{cm^{-1}}$) associated with the NI transition [23,26,31,32] as detailed later.

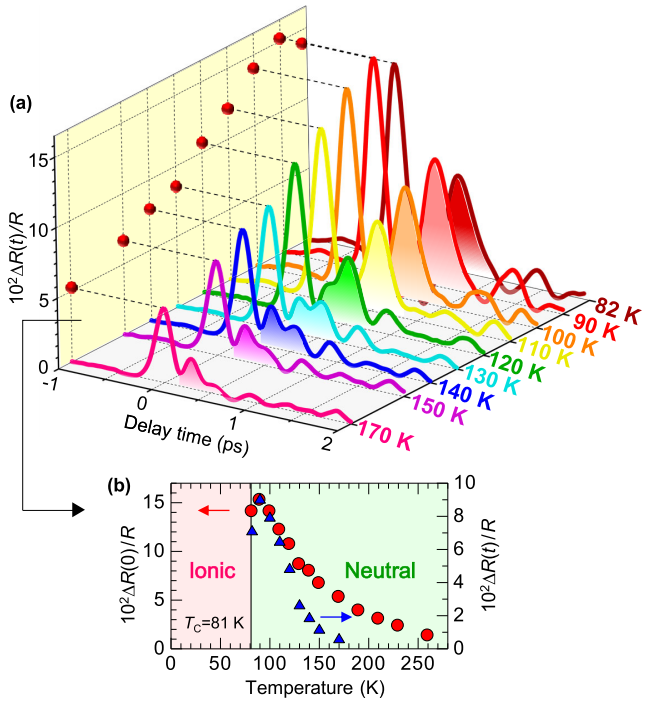

FIG. 2. (a) Time evolutions of terahertz-field-induced reflectivity changes $\Delta R(t)/R$ at various temperatures. (b) Temperature dependence of the first and the second peak structures (circles and triangles, respectively). The terahertz electric-field waveform $[E_{\mathrm{THz}}(t)]$ is shown in Fig. 1(e).

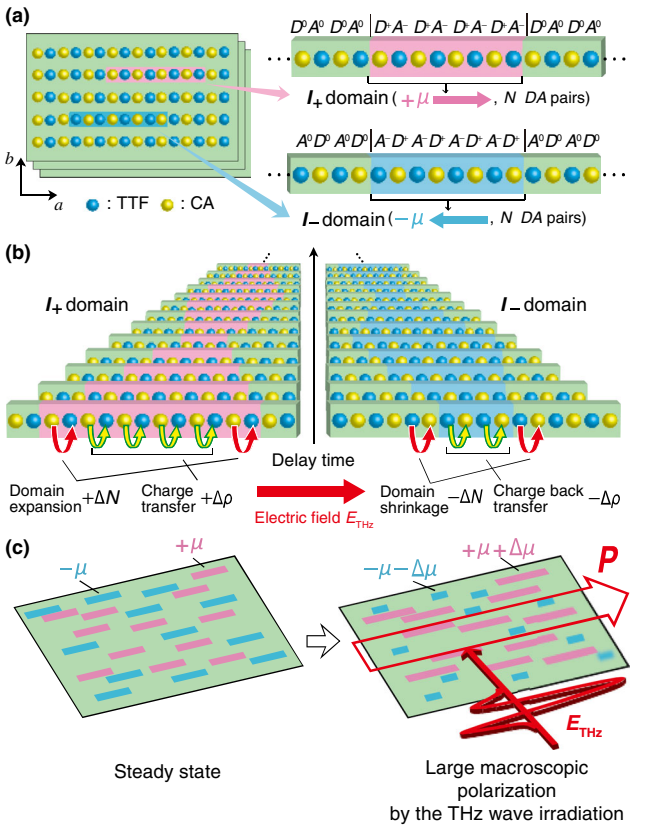

FIG. 3. (a) An I_+ domain with a dipole moment $+\mu$ and an I_- domain with a dipole moment $-\mu$, which are generated in the neutral phase. In the right figures, ρ values are expressed as ± 1 for simplicity. (b) Time evolutions of 1D ionic domains. The terahertz electric field increases (decreases) the size of the $I_+(I_-)$ domain via intermolecular CTs (red curved arrows) and changes ρ by $\Delta\rho(-\Delta\rho)$ within the ionic domain (yellow curved arrows). Subsequently, coherent oscillations of NIDW pairs occur. (c) The large macroscopic polarization produced by microscopic change of 1D ionic domains.

To interpret the anomalous temperature dependence of $\Delta R(t)/R$, we consider microscopic 1D ionic domains as shown in Figs. 3(a) and 3(b). Previous experimental studies [33–36] suggest that such ionic domains are generated even in the neutral phase because of the valence instability, and fluctuated in time and space. In the present study, we performed the infrared molecular vibrational spectroscopy to evaluate the amounts of ionic domains and revealed that about 20% of molecules are ionized and exist as ionic domains at 90 K just above T_c (Supplemental Material S3 [27]).

Here, we simply consider two ionic domains I_+ and I_- with opposite directions of dipole-moments, $+\mu$ and $-\mu$, respectively [Fig. 3(a)]. The moment μ is large, since an ionic domain consists of approximately ten DA pairs [31,36]. In the absence of electric field, $+\mu$ and $-\mu$ cancel. When applying a right-handed field, a fractional CT occurs in each DA pair, increasing (decreasing) ρ_I by $\Delta\rho$ within the $I_+(I_-)$ domain. Although a finite dipole moment is generated, the changes in ρ in the two ionic domains ($\pm\Delta\rho$) also cancel, which does not agree with the experimental result.

The observed field-induced increases in the total values of ρ and μ can be explained in terms of the motions of domain walls between the neutral and ionic states, which are called neutral-ionic domain walls (NIDWs). The quantum mechanical dynamics of NIDWs was theoretically studied by Nagaosa and Takimoto [37]. When the neutral and ionic states are almost degenerate, an ionic domain is regarded as an excitation of an NIDW pair. Just above T_c, TTF-CA shows the anomalous increases of the dielectric response and the nonlinear electronic current, which are interpreted as being due to motions of NIDWs [33,35]. If the I_+ domain, polarized parallel to $E_{\mathrm{THz}}(0)$, expands and the I_- domain, polarized antiparallel to $E_{\mathrm{THz}}(0)$ shrinks as shown in Fig. 3(b), the total values of ρ and μ increase. Such microscopic changes of μ in a number of ionic domains generate the large macroscopic polarization [the right panel of Fig. 3(c)]. Indeed, the $\Delta I_{\mathrm{SHG}}(t)$ and $\Delta R(t)/R$ responses around $t = 0$ follow the changes of $[E_{\mathrm{THz}}(t)]^2$ on the subpicosecond time scale accurately [Figs. 1(f) and 1(g)], suggesting that the initial NIDW motions are purely electronic processes brought about by the intermolecular CTs.

Based on the qualitative interpretations of the results presented above, we can derive a formula for $\Delta R(t)/R$. When the electric field is applied, the number of DA pairs included in the ionic domain, N (the domain size), changes as $N \to N + \Delta N$ (or $N \to N - \Delta N$) and ρ changes as

$\rho \to \rho_I + \Delta\rho$ (or $\rho \to \rho_I - \Delta\rho$) in the I_+ (or I_-) domain. Assuming that ΔR is proportional to the change in the total value of ρ within ionic domains, we obtain the following relation:

$$\Delta R \propto \frac{1}{2}[(N+\Delta N)(\rho_I+\Delta\rho)+(N-\Delta N)(\rho_I-\Delta\rho)-2\rho N] = \Delta\rho\Delta N \quad (1)$$

The enhancement of $\Delta R(0)/R$ as the temperature approaches T_c [Fig. 2(a)] can be attributed to the increase in the number of 1D ionic domains and/or to the increase in ΔN originating from the enhancement of the valence instability. Both $\Delta\rho(0)$ and $\Delta N(0)$ are proportional to $E_{\mathrm{THz}}(0)$, resulting in $\Delta R(t)/R \propto [E_{\mathrm{THz}}(t)]^2$ around $t = 0$ as observed in the experiments.

The subsequent oscillatory responses observed in $\Delta I_{\mathrm{SHG}}(t)$ and $\Delta R(t)/R$ can be attributed to the breathing oscillation of NIDW pairs. After the initial rapid NIDW motions by CT processes, the altered ionic domains are stabilized by molecular displacements within a few picoseconds. In the photoinduced neutral-to-ionic transition in TTF-CA [23,38], such transient molecular displacements are also observed [26,31]. The molecular displacements slow down the breathing oscillation of NIDW pairs and decrease its frequency into the terahertz region. Assuming that $\Delta\rho(t)$ is proportional to $E_{\mathrm{THz}}(t)$ and $\Delta N(t)$ is forced by $E_{\mathrm{THz}}(t)$ to oscillate in a quantum-mechanical sense, $\Delta R(t)$ is expressed as

$$\Delta R(t) \propto E_{\mathrm{THz}}(t)\int_{-\infty}^{t} E_{\mathrm{THz}}(\tau)e^{-(t-\tau)/\tau_0}\cos[\omega(t-\tau)+\phi]d\tau. \quad (2)$$

The integral in Eq. (2) expresses the time progression of $\Delta N(t)$. The parameters τ_0, ω, and ϕ are the decay time, the frequency, and the initial phase of the oscillation, respectively. In Fig. 4(a), we show the simulated curve at 140 K (solid line), which reproduces well the experimental result (circles). The parameter values used were $\omega = 28\ \mathrm{cm}^{-1}$, $\tau_0 = 0.9$ ps, and $\phi = 5 \pm 5°$. The phase ϕ is almost equal to 0, indicating that the oscillation is cosinusoidal, consistent with the instantaneous initial NIDW motions. The lower panels show $\Delta\rho(t)[\propto E_{\mathrm{THz}}(t)]$ and $\Delta N(t)$. In addition to the quantum motions of NIDWs expressed by Eq. (2), we detect another coherent oscillation, with a frequency of 54 cm^{-1}, related to the dimerization [23,26,31]. The contribution of this oscillation is described in Supplemental Material S4 [27].

The time progression of $\Delta R(t)/R$ at various temperatures can also be reproduced by Eq. (2) with $\phi \sim 0$, as shown in Fig. 4(b), for example. The obtained values for ω and τ_0 are plotted against temperature in Fig. 4(c). With decreasing temperature, ω decreases from 30 to 20 cm^{-1} and τ_0 increases from 0.5 to 3 ps. These behaviors are

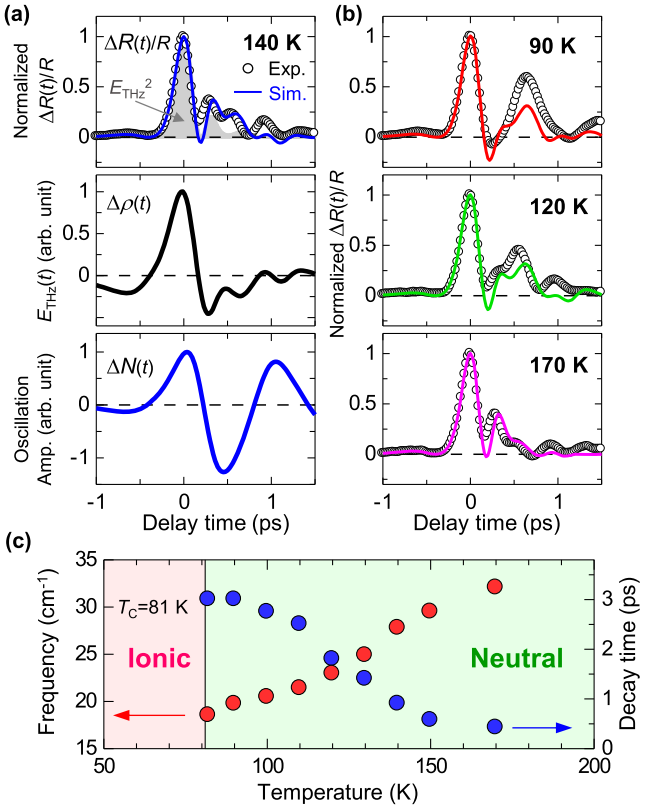

FIG. 4. (a) Normalized time evolutions of $\Delta R(t)/R$, $\Delta\rho(t)$ [$\propto E_{\mathrm{THz}}(t)$], and $\Delta N(t)$ at 140 K. The solid line in the top panel is a fitting curve. (b) Typical simulation results of $\Delta R(t)/R$ with the fitting curves (solid lines). (c) Temperature dependence of the frequency ω and the decay time τ_0 of the NIDW oscillation.

explained by the fact that the energy difference between the neutral and ionic states decreases on approaching T_c. In the steady-state infrared spectroscopy, several modes are detected below 100 cm^{-1} and a mode shows a softening from 52 cm^{-1} at 200 K to 19 cm^{-1} just above T_c [39–41]. However, the complicated time progressions of $\Delta R(t)/R$ shown in Fig. 2(a) cannot be reproduced with any simple vibration mode. In the steady-state infrared spectra, the oscillation of NIDWs might be obscured by the other infrared-active modes.

Based upon the above-mentioned model, we can evaluate the magnitudes of the field-induced changes in ρ and the size of an ionic domain. By analyzing the time dependence of $\Delta I_{\mathrm{SHG}}(t)$ and the magnitude of $\Delta I_{\mathrm{SHG-90\ K}}(0)/I_{\mathrm{SHG-65\ K}}$, we can determine $\Delta\rho$ and $\Delta N/N$ (Supplemental Material S5 [27]). At $E_{\mathrm{THz}}(0) =$ 415 kV/cm and at 90 K, we obtain $\Delta\rho \sim 0.085$ $(\Delta\rho/\rho_N \sim 0.27)$ and $\Delta N/N \sim 0.43$. Namely, the terahertz electric-field pulse increases ρ by ~27% and the ionic-domain size by ~43%. Such large changes can be attributed to the enhanced valence instability just above T_c and are responsible for the formation of the large macroscopic polarization reaching 17% of that in the ferroelectric ionic phase. This initial response can be considered a kind of third-order optical

nonlinearity. However, we would like to emphasize that the observed phenomenon is completely different from conventional third-order optical nonlinearity characterized by coherent electronic processes, since the former includes real intermolecular CTs and molecular dynamics.

In summary, large macroscopic polarization can be generated by a terahertz electric-field pulse in the paraelectric neutral phase of TTF-CA. The mechanism for the polarization generation is explained by the quantum dynamics of NIDW pairs via field-induced intermolecular CTs. The field-induced large polarization is attributed not only to the strong instability to the ionic state, but also the electronic dielectricity based upon the directional intermolecular CTs. We also succeeded in detecting breathing motions of NIDW pairs. This is crucial since the NIDW dynamics dominate dielectric and transport properties in the donor-acceptor-type molecular compounds. A real time detection of such domain-wall dynamics has been difficult to be achieved by the other methods. Thus, the results presented here demonstrate the high potential of our method using a terahertz pulse for clarifying the nature of ferroelectric domain walls as well as for generating large macroscopic polarizations. This approach can also be applied to various organic and inorganic materials displaying valence instabilities or charge fluctuations, and will assist the discovery of new nonequilibrium electronic phases and domain-wall dynamics in electric fields.

This work was partly supported by Grants-in-Aid for Scientific Research from the Japan Society for the Promotion of Science (JSPS) (Projects No. 25247049, No. 25247058, and No. 15H03549), and CREST, Japan Science and Technology Agency. T. Morimoto, H. Yamakawa, and T. Terashige were supported by the JSPS through the Program for Leading Graduate Schools (MERIT).

[1] T. Kampfrath, K. Tanaka, and K. A. Nelson, Nat. Photonics **7**, 680 (2013).
[2] H. Y. Hwang, S. Fleischer, N. C. Brandt, B. G. Perkins Jr, M. Liu, K. Fan, A. Sternbach, X. Zhang, R. D. Averitt, and K. A. Nelson, J. Mod. Opt. **62**, 1447 (2015).
[3] T. Kampfrath, A. Sell, G. Klatt, A. Pashkin, S. Mahrlei1, T. Dekorsy, M. Wolf, M. Fiebig, A. Leitenstorfer, and R. Huber, Nat. Photonics **5**, 31 (2011).
[4] H. Hirori, K. Shinokita, M. Shirai, S. Tani, Y. Kadoya, and K. Tanaka, Nat. Commun. **2**, 594 (2011).
[5] I. Katayama, H. Aoki, J. Takeda, H. Shimosato, M. Ashida, R. Kinjo, I. Kawayama, M. Tonouchi, M. Nagai, and K. Tanaka, Phys. Rev. Lett. **108**, 097401 (2012).
[6] M. Liu, H. Y. Hwang, H. Tao, A. C. Strikwerda, K. Fan, G. R. Keiser, A. J. Sternbach, K. G. West, S. Kittiwatanakul, J. Lu, S. A. Wolf, F. G. Omenetto, X. Zhang, K. A. Nelson, and R. D. Averitt, Nature (London) **487**, 345 (2012).
[7] H. Yada, T. Miyamoto, and H. Okamoto, Appl. Phys. Lett. **102**, 091104 (2013).
[8] T. Miyamoto, H. Yada, H. Yamakawa, and H. Okamoto, Nat. Commun. **4**, 2586 (2013).
[9] C. Vicario, C. Ruchert, F. Ardana-Lamas, P. M. Derlet, B. Tudu, J. Luning, and C. P. Hauri, Nat. Photonics **7**, 720 (2013).
[10] T. Kubacka *et al.*, Science **343**, 1333 (2014).
[11] R. Matsunaga, N. Tsuji, H. Fujita, A. Sugioka, K Makise, Y. Uzawa, H. Terai, Z. Wang, H. Aoki, and R. Shimano, Science **345**, 1145 (2014).
[12] F. Chen, J. Goodfellow, S. Liu, I. Grinberg, M. C. Hoffmann, A. R. Damodaran, Y. Zhu, P. Zalden, X. Zhang, I. Takeuchi, A. M. Rappe, L. W. Martin, H. Wen, and A. M. Lindenberg, Adv. Mater. **27**, 6371 (2015).
[13] H. Yamakawa, T. Miyamoto, T. Morimoto, H. Yada, Y. Kinoshita, M. Sotome, N. Kida, K. Yamamoto, K. Iwano, Y. Matsumoto, S. Watanabe, Y. Shimoi, M. Suda, H. M. Yamamoto, H. Mori, and H. Okamoto, Sci. Rep. **6**, 20571 (2016).
[14] J. B. Torrance, J. E. Vazquez, J. J. Mayerle, and V. Y. Lee, Phys. Rev. Lett. **46**, 253 (1981).
[15] H. M. McConnell, B. M. Hoffman, and R. M. Metzger, Proc. Natl. Acad. Sci. U.S.A. **53**, 46 (1965).
[16] J. B. Torrance, A. Girlando, J. J. Mayerle, J. I. Crowley, V. Y. Lee, P. Batail, and S. J. LaPlaca, Phys. Rev. Lett. **47**, 1747 (1981).
[17] M. Le Cointe, M. H. Lemée-Cailleau, H. Cailleau, B. Toudic, L. Toupet, G. Heger, F. Moussa, P. Schweiss, K. H. Kraft, and N. Karl, Phys. Rev. B **51**, 3374 (1995).
[18] S. Horiuchi, Y. Okimoto, R. Kumai, and Y. Tokura, J. Phys. Soc. Jpn. **69**, 1302 (2000).
[19] K. Kobayashi, S. Horiuchi, R. Kumai, F. Kagawa, Y. Murakami, and Y. Tokura, Phys. Rev. Lett. **108**, 237601 (2012).
[20] G. Giovannetti, S. Kumar, A. Stroppa, J. van den Brink, and S. Picozzi, Phys. Rev. Lett. **103**, 266401 (2009).
[21] S. Ishibashi and K. Terakura, Physica **405B**, S338 (2010).
[22] T. Portengen, Th. Östreich, and L. J. Sham, Phys. Rev. B **54**, 17452 (1996).
[23] H. Okamoto, Y. Ishige, S. Tanaka, H. Kishida, S. Iwai, and Y. Tokura, Phys. Rev. B **70**, 165202 (2004).
[24] J. Hebling, G. Almási, I. Z. Kozma, and J. Kuhl, Opt. Express **10**, 1161 (2002).
[25] T. Luty, H. Cailleau, S. Koshihara, E. Collet, M. Takesada, M. H. Lemée-Cailleau, M. Buron-Le Cointe, N. Nagaosa, Y. Tokura, E. Zienkiewicz, and B. Ouladdiaf, Europhys. Lett. **59**, 619 (2002).
[26] S. Iwai, Y. Ishige, S. Tanaka, Y. Okimoto, Y. Tokura, and H. Okamoto, Phys. Rev. Lett. **96**, 057403 (2006).
[27] See Supplemental Material at http://link.aps.org/supplemental/10.1103/PhysRevLett.118.107602, which includes Refs. [28–30], for the terahertz-electric-field dependence of reflectivity changes, the details of the probe-energy dependence of the reflectivity changes by terahertz electric fields, the estimation of the amount of ionic domains in the neutral phase, the coherent oscillation of the lattice mode, and the analyses of time characteristics of the terahertz-field-induced SHG.
[28] H. Matsuzaki, H. Takamatsu, H. Kishida, and H. Okamoto, J. Phys. Soc. Jpn. **74**, 2925 (2005).

[29] A. Painelli and A. Girlando, J. Chem. Phys. **84**, 5655 (1986).
[30] C. Katan, J. Phys. Chem. A **103**, 1407 (1999).
[31] H. Uemura and H. Okamoto, Phys. Rev. Lett. **105**, 258302 (2010).
[32] T. Miyamoto, H. Uemura, and H. Okamoto, J. Phys. Soc. Jpn. **81**, 073703 (2012).
[33] Y. Tokura, H. Okamoto, T. Koda, T. Mitani, and G. Saito, Phys. Rev. B **38**, 2215 (1988).
[34] Y. Tokura, S. Koshihara, Y. Iwasa, H. Okamoto, T. Komatsu, T. Koda, N. Iwasawa, and G. Saito, Phys. Rev. Lett. **63**, 2405 (1989).
[35] H. Okamoto, T. Mitani, Y. Tokura, S. Koshihara, T. Komatsu, Y. Iwasa, T. Koda, and G. Saito, Phys. Rev. B **43**, 8224 (1991).
[36] M. Buron-Le Cointe, M. H. Lemée-Cailleau, H. Cailleau, S. Ravy, J. F. Bérar, S. Rouzière, E. Elkaïm, and E. Collet, Phys. Rev. Lett. **96**, 205503 (2006).
[37] N. Nagaosa and J. Takimoto, J. Phys. Soc. Jpn. **55**, 2745 (1986).
[38] E. Collet, M. H. Cailleau, M. B. Cointe, H. Cailleau, M. Wulff, T. Luty, S. Koshihara, M. Meyer, L. Toupet, P. Rabiller, and S. Techert, Science **300**, 612 (2003).
[39] A. Moreac, A. Girard, Y. Delugeard, and Y. Marqueton, J. Phys. Condens. Matter **8**, 3553 (1996).
[40] M. Masino, A. Girlando, and Z. G. Soos, Chem. Phys. Lett. **369**, 428 (2003).
[41] A. Girlando, M. Masino, A. Painelli, N. Drichko, M. Dressel, A. Brillante, R. G. Della Valle, and E. Venuti, Phys. Rev. B **78**, 045103 (2008).